17th World Conference on Earthquake Engineering, 17WCEE
Sendai, Japan - September 13th to 18th 2020

ESTIMATION OF THE SHORT-PERIOD LEVEL OF THE 2011 OFF THE PACIFIC COAST OF TOHOKU EARTHQUAKE BY STOCHASTIC GREEN'S FUNCTION METHOD

D. Ju [1], K. Arai[2], K. Dan[3], H. Fujiwara[4], and N. Morikawa[5]

[1] *Ohsaki Research Institute, Inc., Japan, judianshu@ohsaki.co.jp*
[2] *Shimizu Corporation, Japan, arai@shimz.co.jp*
[3] *Ohsaki Research Institute, Inc., Japan, dan@ohsaki.co.jp*
[4] *National Research Institute for Earth Science and Disaster Resilience, Japan, fujiwara@bosai.go.jp*
[5] *National Research Institute for Earth Science and Disaster Resilience, Japan, morikawa@bosai.go.jp*

Abstract

In Japan, strong motion predictions are usually carried out in accordance with the official procedure, so called Recipe, published by the Headquarters for Earthquake Research Promotion, Japan (2005). The short-period level, which is the flat level of the acceleration source spectrum in the short-period range, plays an important role in the Recipe, because it controls the amplitudes of short-period ground motions.

The 2011 off the Pacific coast of Tohoku earthquake was the first M_W 9-class event that provided with plenty of strong ground motion records and that enabled us to assess the short-period level of an M_W 9-class event. For example, the SMGA (Strong Motion Generation Area) models obtained by Satoh (2012), Kawabe and Kamae (2013), and Kurahashi and Irikura (2013) using the empirical Green's function method provide with the short-period level of 3.51 E+20 Nm/s^2, 1.80 E+20 Nm/s^2, and 1.78 E+20 Nm/s^2, respectively. These values are one to two times of that in the empirical relationship between the seismic moment and the short-period level established for crustal earthquakes.

This paper aims to facilitate the broadband ground motion prediction of future M_W 9-class events along Japan trench, Nankai trough, Sagami trough, and Kuril trench, by estimating the short-period level for the 2011 Tohoku earthquake based on the SMGA model using the stochastic Green's function method.

For that, firstly, we adopted two source models, which were the SMGA model of case 1 based on Kawabe and Kamae (2013) and the SMGA model of case 2 with larger value of the short-period level than that of case 1 by referring to Satoh (2012). Secondly, we calculated strong motions at three KiK-net stations (in Miyagi-ken, Fukushima-ken, and Ibaraki-ken) by the stochastic Green's function method and examined which of the two SMGA models reproduced the records better. The results showed that the latter of the two cases had a better fit. Furthermore, we examined how well the SMGA models reproduced the seismic intensity distribution. At locations, where the seismic intensities calculated from the simulated waveforms were greater than 6, the SMGA model of case 2 overestimated the recorded seismic intensities. Finally, the intermediate source model between the above two SMGA models was set as case 3, and its strong motions were calculated. The simulation results reproduced the recorded data well in terms of the strong motions at the three KiK-net stations and the seismic intensity distribution. The short-period level for case 3 was 2.36 E+20 Nm/s^2, 1.3 times larger than the empirical relationship between the seismic moment and the short-period level established for crustal earthquakes.

Keywords: 2011 off the Pacific coast of Tohoku earthquake, short-period level, stochastic Green's function method

1. Introduction

The prediction of strong motions for earthquake resistant design of buildings and structures in Japan is usually carried out in accordance with the official procedure, so called Recipe, published by the Headquarters for Earthquake Research Promotion, Japan (2005)[1]. According to the Recipe, the short-period level of the source plays an important role for the earthquake resistant design, because the short-period level controls the amplitude of ground motions in the periods shorter than few seconds. The short-period level, which is the flat level of the acceleration source spectrum in the short-period range, usually estimated by the empirical relationship with the seismic moment by Dan *et al*. (2001)[2].

Meanwhile, the 2011 off the Pacific coast of Tohoku earthquake was the first M_W 9-class event that provided with plenty of strong ground motion records. The short-period level for this event was assessed by several studies (e.g. Satoh, 2012; Kawabe and Kamae, 2013; Kurahashi and Irikura, 2013)[3]-[5]. Those values were one to two times of that in the empirical relationship between the seismic moment and the short-period level established for crustal earthquakes by Dan *et al*. (2001)[2], and they were estimated from SMGA (Strong Motion Generation Area) models obtained by the empirical Green's function method. Sometimes, different values of the short-period level are assessed for the same earthquake (Satoh, 2010)[6]. The estimates of the short-period level may vary, which can be caused by difference in short-period level estimates of small earthquakes used as Green's functions in empirical Green's function method, or by selection of a reference site in spectral inversions.

On the other hand, for ground motion prediction in a wide region by the Headquarters for Earthquake Research Promotion, Japan (2004)[7], the short-period components are usually calculated by the stochastic Green's function method.

Therefore, this paper aims to facilitate the broadband ground motion prediction of future M_W 9-class events along Japan trench, Nankai trough, Sagami trough, and Kuril trench, by estimating the short-period level for the 2011 off the Pacific coast of Tohoku earthquake based on the SMGA model using the stochastic Green's function method. For that, firstly, we adopted two source models, which were the SMGA model of case 1 based on Kawabe and Kamae (2013)[4] and the SMGA model of case 2 based on Satoh (2012)[3] with larger value of the short-period level. Secondly, we calculated strong motions at three KiK-net stations (in Miyagi-ken, Fukushima-ken, and Ibaraki-ken) by the stochastic Green's function method and examined suitability of the two SMGA models. Furthermore, we examined how well the SMGA models reproduced the seismic intensity distribution. For that we compared the seismic intensities for the K-NET, KiK-net, and JMA stations calculated from the stochastic Green's function method results with those of the observed strong motions. Finally, based on the results of the two SMGA models, we proposed an intermediate source model between the above two SMGA models, and examined how well it reproduced the strong motion records at the three KiK-net stations and the observed seismic intensity distribution using the stochastic Green's function method.

2. Fault models for the 2011 off the Pacific coast of Tohoku earthquake based on the SMGA models

2.1 Short-period level

Satoh (2012)[3], Kawabe and Kamae (2013)[4], and Kurahashi and Irikura (2013)[5] proposed SMGA (Strong Motion Generation Area) models for the 2011 off the Pacific coast of Tohoku earthquake. These models were all obtained by using the empirical Green's function method. The short-period levels can be calculated from the area S_i and stress drop $\Delta\sigma_i$ of each SMGA by the following equations:

$$A = \left(\sum_{i=1}^{n} A_i^2 \right)^{1/2}, \quad (1)$$

$$A_i = 4\pi\beta^2 \Delta\sigma_i (S_i / \pi)^{1/2} . \quad (2)$$

Here, i is the assigned number of the each SMGA, n is the total number of the SMGAs, and β is the *S*-wave velocity at the source. The calculated short-period levels of the SMGA models by Satoh (2012)[3], Kawabe and Kamae (2013)[4], and Kurahashi and Irikura (2013)[5] are 3.51 E+20 Nm/s^2, 1.80 E+20 Nm/s^2, and 1.78 E+20 Nm/s^2, respectively. Here, we assumed the *S*-wave velocity β to be 4.0 km/s (Yoshida *et al*., 2011)[8].

According to the CMT solution by the Japan Meteorological Agency, the seismic moment of the 2011 off the Pacific coast of Tohoku earthquake is 4.22E+22 Nm. Using this value, we calculated the short-period level from the empirical relationship between seismic moment and short-period level established for crustal earthquakes (Dan *et al*., 2001)[2] to be 1.85 E+20 Nm/s^2. As a result, the short-period level of the SMGA model by Satoh (2012)[3] is two times larger than that from the empirical relationship established for crustal earthquakes. The values for Kawabe and Kamae (2013)[4] and Kurahashi and Irikura (2013)[5] models are consistent with the empirical relationship for crustal earthquakes.

The difference in the short-period levels could be caused by the different estimates of short-period levels of small earthquakes, which are used as the Green's functions in the empirical Green's function method. For example, the short-period level for October 9, 2005 earthquake (M_W 6.3), the Green's function in Kawabe and Kamae (2013)[4], was calculated 8.32E+18 Nm/s^2 from the corner frequency, but it was estimated 1.21E+19 Nm/s^2 by Satoh (2012)[3] from the spectral inversion, which is about 1.5 times larger value.

2.2 SMGA model of case 1 based on Kawabe and Kamae (2013)[4]

We set an initial SMGA model (hereafter case 1) for the 2011 off the Pacific coast of Tohoku earthquake based on Kawabe and Kamae (2013)[4]. In this model, the SMGA areas were adopted from the SMGA model by Kawabe and Kamae (2013)[4]. The stress drops of the SMGAs were set to be 10 to 25 MPa, which were adopted from Kawabe and Kamae (2013)[4] as well.

We assumed the values for the *S*-wave velocity β at the source as 4.0 km/s from Yoshida *et al*. (2011)[8], and the density as 3.0 g/cm^3 from the *S*-wave velocity and density relationship by Ludwig *et al*. (1970)[9]. For the SMGA locations, rupture initiation locations, and rupture timing, we referred to Kawabe and Kamae (2013)[4].

Table 1 lists the fault parameters, and Figure 1 illustrates the fault model for the SMGA model of case 1. The short-period level of the case 1 is 1.75E+20 Nm/s^2, which is 0.9 times of the empirical relation for crustal earthquakes.

2.3 SMGA model of case 2 based on Satoh (2012)[3]

Here, we set another SMGA model (hereafter case 2) for the 2011 off the Pacific coast of Tohoku earthquake based on Satoh (2012)[3]. In this model, the SMGA areas, SMGA locations, rupture initiation locations, and rupture timing were the same as in the case 1, with only change in the stress drops of SMGA's, which are set to be a higher value of 20 to 40 MPa.

Table 1 – Parameters of the SMGA model of case 1

SMGA	area S_i (km^2)	seismic moment M_0 (Nm)	slip D_i (m)	stress drop $\Delta\sigma_i$ (MPa)	short-period level A_i (N·m/s^2)
SMGA1	1600	5.25E+20	6.8	20	9.07E+19
SMGA2	2500	1.03E+21	8.6	20	1.13E+20
SMGA3	400	4.93E+19	2.6	15	3.40E+19
SMGA4	900	1.11E+20	2.6	10	3.40E+19
SMGA5	900	2.77E+20	6.4	25	8.51E+19
total					1.75E+20

Table 2 – Parameters of the SMGA model of case 2

SMGA	area S (km^2)	seismic moment M_0 (Nm)	slip D (m)	stress drop $\Delta\sigma$ (MPa)	short-period level A (N·m/s^2)
SMGA1	1600	1.05E+21	13.7	40	1.81E+20
SMGA2	2500	1.28E+21	10.7	25	1.42E+20
SMGA3	400	6.57E+19	3.4	20	4.54E+19
SMGA4	900	2.22E+20	5.1	20	6.81E+19
SMGA5	900	3.32E+20	7.7	30	1.02E+20
total					2.65E+20

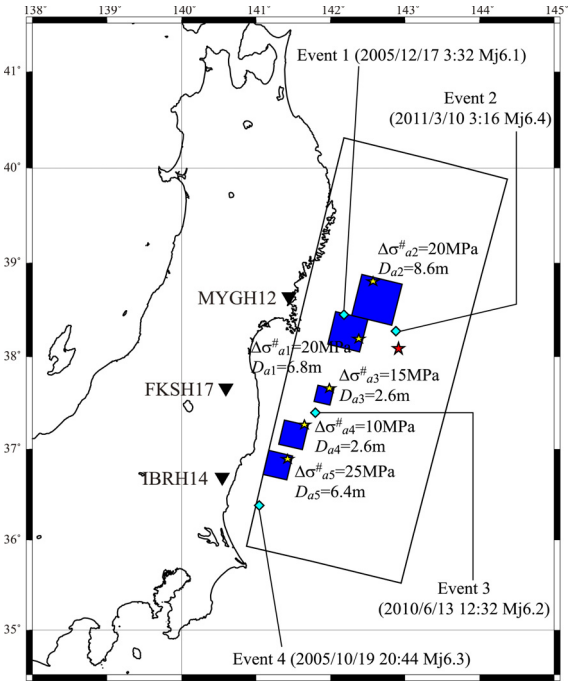

Fig. 1 – SMGA model of case 1 for the 2011 Tohoku earthquake and the locations of the ground motion simulation stations. This SMGA model is based on Kawabe and Kamae (2013)[4].

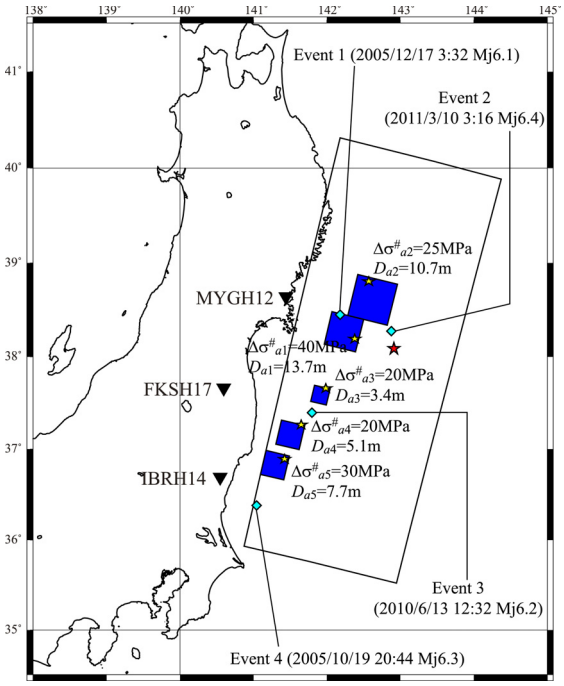

Fig. 2 – SMGA model of case 2 for the 2011 Tohoku earthquake and the locations of the ground motion simulation stations. The stress drops on the SMGA's are modified from case 1 in reference to Satoh (2012)[3].

Table 2 lists the fault parameters, and Figure 2 illustrates the fault model for the SMGA model of case 2. The short-period level of the case 2 is 2.65E+20 Nm/s^2, which is 1.4 times of the empirical relation for crustal earthquakes.

3. Reproducing strong ground motion recordings by the stochastic Green's function method

3.1 Stochastic Green's function method

We calculated strong ground motions at three representative KiK-net stations, which are MYGH12 (Miyagi-ken), FKSH17 (Fukushima-ken), and IBRH14 (Ibaraki-ken), by using the stochastic Green's function method by Dan *et al*. (2010)[10]. For the generation of the stochastic Green's functions, we used the envelope time function by Boore (1983)[11]. The f_{max} was fixed at 11 Hz as in Satoh (2013)[12] for the 2011 off the Pacific coast of Tohoku earthquake. The transition frequency range of radiation pattern correction between theoretical coefficients and average of theoretical radiation pattern values over all azimuths and ranges of takeoff angles was from 3 to 6 Hz. The quality factor was $Q(f)=154\,f^{0.91}$ for $f \geqq 0.5$ Hz and $Q=82$ for $f < 0.5$ Hz, based on the analysis results of Satoh (2007)[13] for the records of subduction plate-boundary earthquakes in the Pacific coast of the east Japan.

Figures 1 and 2 also show the location of the Event 1 to Event 4, which were used by Kawabe and Kamae (2013)[4] as the empirical Green's functions. We created stochastic Green's functions at the same locations and of the same seismic moment magnitudes as the empirical Green's functions for Event 1 to Event 4 in Kawabe and Kamae (2013)[4], using the same fault parameters as in Kawabe and Kamae (2013)[4]. For that, we generated the waves on the seismogenic layer, and then, based on the one-dimensional wave propagation theory created the stochastic Green's functions at the bore-hole level of each station, which is the same level as the records of the 2011 off the Pacific coast of Tohoku earthquake.

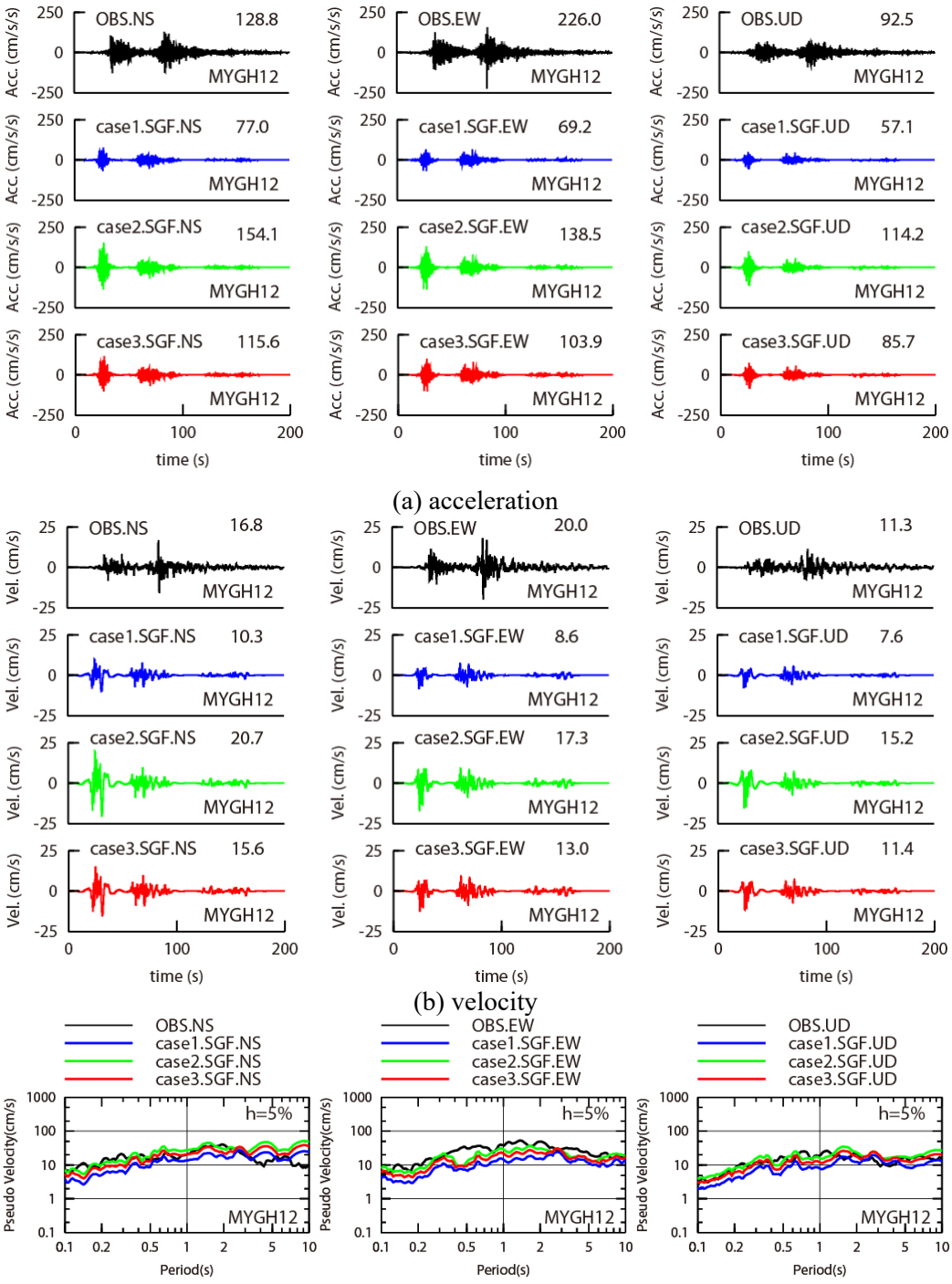

Fig. 3 – Comparison of the calculated strong ground motions at MYGH12 by the stochastic Green's function method with the observation.

3.2 Strong ground motion calculation results

Figures 3 to 5 compare the accelerations, velocities, and pseudo velocity response spectra with the damping factor of 5% of the simulated strong motions by the stochastic Green's function method for the SMGA model of case 1 and the SMGA model of case 2 with those of the observed strong motions. In the figures, the observed strong motions and the results of cases 1 and 2 are plotted in black, blue, and green, respectively.

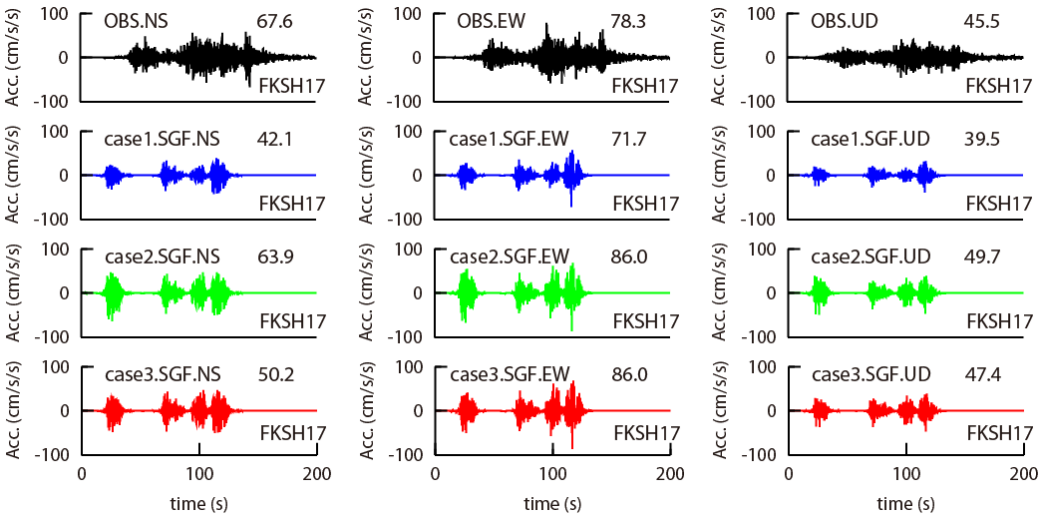

(a) acceleration

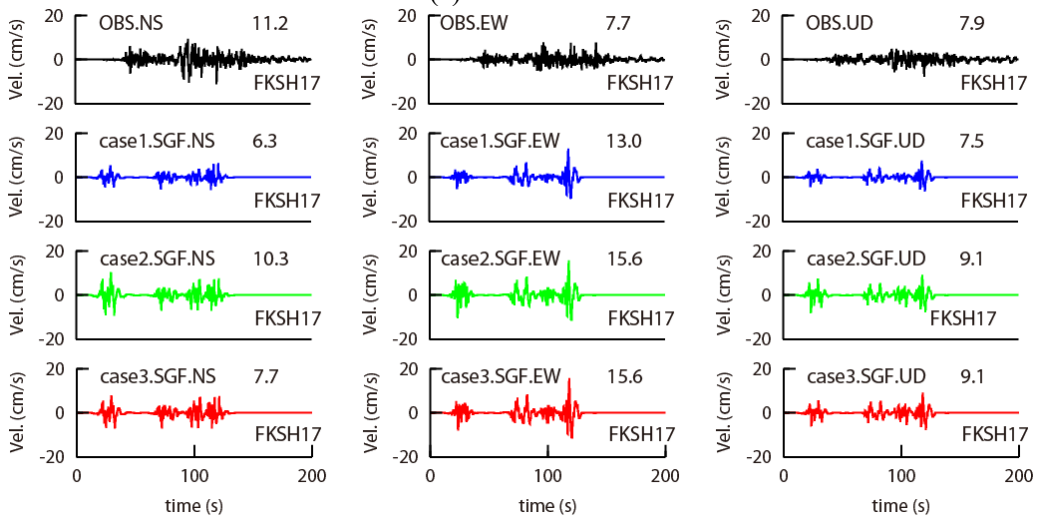

(b) velocity

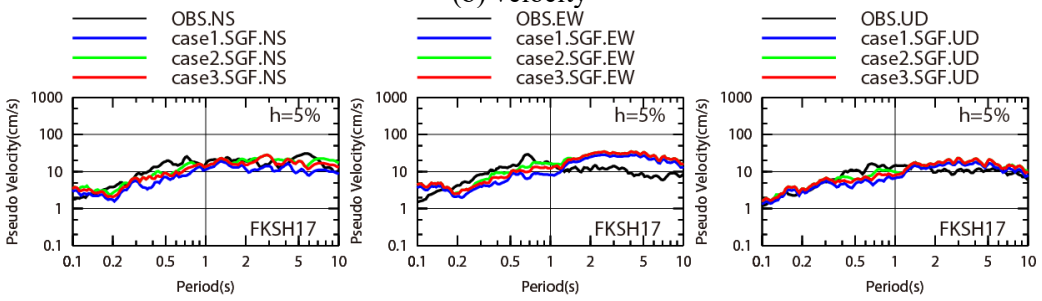

(c) pseudo velocity response spectra

Fig. 4 – Comparison of the calculated strong ground motions at FKSH17 by the stochastic Green's function method with the observation.

For the SMGA model of case 1, the peak accelerations (Fig. 3 (a)) and peak velocities (Fig. 3 (b)) of the simulated strong ground motions are smaller than those of the observed records at MYGH12 station for all three components. Also, the pseudo velocity response spectra (Fig. 3 (c)) are underestimated for all the three components at periods shorter than 1 second. At FKSH17 and IBRH14 stations, most of the peaks of the simulated accelerations (Fig. 4 (a), Fig. 5 (a)), velocities (Fig. 4 (b), Fig. 5 (b)), and the pseudo velocity response spectra at periods shorter than 1 second (Fig. 4 (c), Fig. 5 (c)) are slightly smaller than those of the observed records.

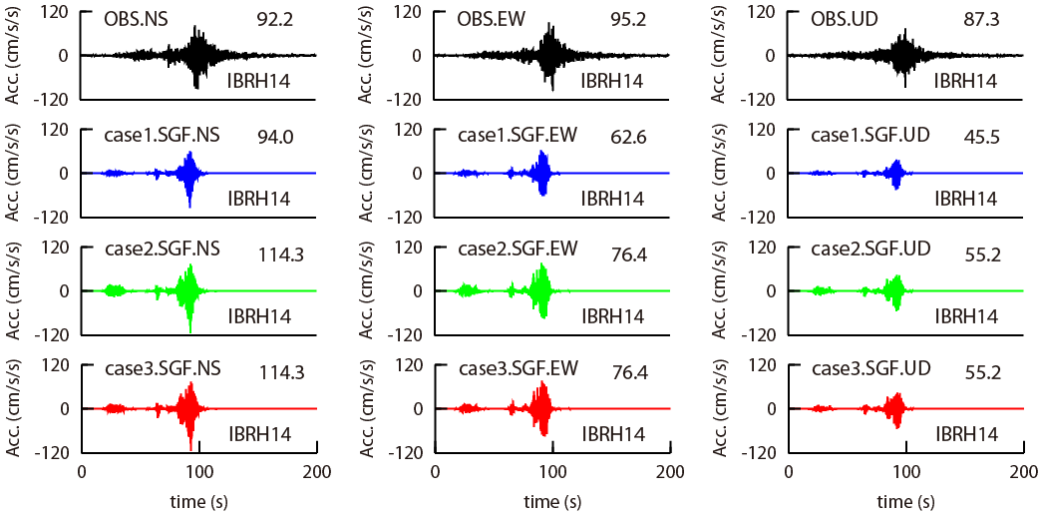

(a) acceleration

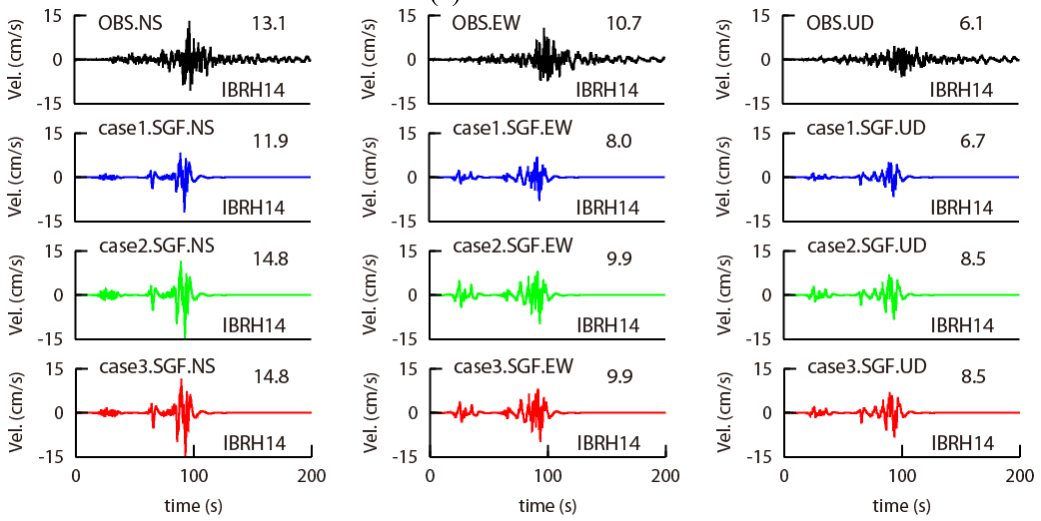

(b) velocity

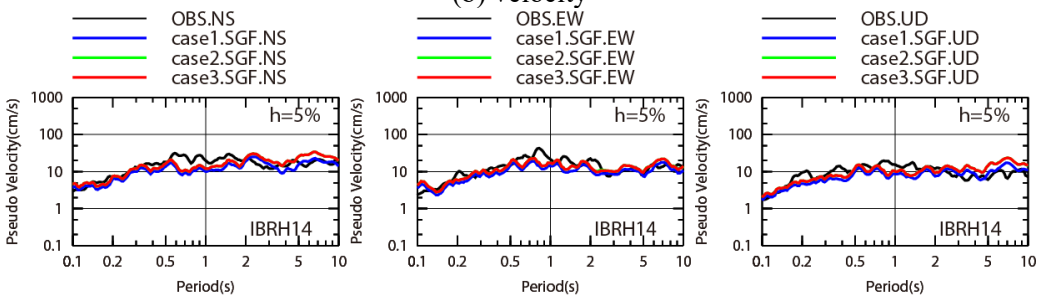

(c) pseudo velocity response spectra

Fig. 5 – Comparison of the calculated strong ground motions at IBRH14 by the stochastic Green's function method with the observation.

For the SMGA model of case 2, the peak accelerations (Fig. 3 (a)) and peak velocities (Fig. 3 (b)) of the simulated strong ground motions are similar to the observed records at MYGH12 station in overall, although the level of similarity is different for each component. The pseudo velocity response spectra of all the three components show better fit to the observed records compared to case 1. Also, at FKSH17 and IBRH14 stations, the peaks of the simulated accelerations (Fig. 4 (a), Fig. 5 (a)) and velocities (Fig. 4 (b), Fig. 5 (b)) have better fit to those of the observed records compared to case 1, and the pseudo velocity response spectra (Fig. 4 (c), Fig. 5 (c)) agree well with those of the observed records.

4. Reproducing seismic intensities

4.1 Calculation method for seismic intensities

We calculated the instrumental seismic intensity distribution from the simulation results by the stochastic Green's function method. In the calculation, we followed the method by the Headquarters for Earthquake Research Promotion, Japan (2017)[14]. For that, we calculated seismic intensities at the ground surface by multiplying the results on the engineering bedrock, which corresponds to a layer with the *S*-wave velocity of 600 m/s, with the AVS-30 amplification factors.

4.2 Calculated seismic intensities

The seismic intensities of the regional simulation results calculated by the stochastic Green's function method are compared with the observed seismic intensities in Figures 6 to 8. The observed seismic intensities were interpolated by the following process: first, we divided the seismic intensities observed on the ground surface at K-NET, KiK-net, and JMA stations (235 points) by the amplification factor of each station, then interpolated the seismic intensities on the engineering bedrock over the study region, and finally, we multiplied the seismic intensities on the engineering bedrock by the amplification factors. The results show that the SMGA model of case 1 underestimated the observed seismic intensities in Iwate-ken and Miyagi-ken, and the SMGA model of case 2 overestimated the observation in this region.

Figures 9 and 10 show the scatter plots of the goodness of fit between simulated and observed seismic intensities for 168 seismic stations out of the 235 stations. In the figures, we removed the stations at Akita-ken, Yamagata-ken, and Chiba-ken due to the far distance from the SMGAs.

In the figures, the dashed lines show ±0.5 standard deviations of the seismic intensities. The results of the case 1 tend to distribute lower than the identity line with the observation, and those of the case 2 seem to distribute almost symmetrically with respect to the observation. We calculated the following *RMSE* (Root Mean Square Error) of the observed seismic intensities and those simulated for the SMGA models of cases 1 and 2:

$$RMSE = \sqrt{[\sum_{i=1}^{N} (Sgf_i - Obs_i)^2]/N} \,. \tag{3}$$

Here, Sgf_i is the simulated seismic intensity at the i-th station, Obs_i is the observed seismic intensity at i-th station, and N is the number of the stations which were used for calculating the seismic intensity distribution.

The *RMSE* of case 1 is 0.58, and the *RMSE* of case 2 is 0.53, which means that the case 2 has smaller deviation than the case 1.

5. Intermediate SMGA model of case 3 for the 2011 Tohoku earthquake

5.1 Fault parameters

The analysis results in Sections 3 and 4 show that the SMGA model of case 1 underestimated both the time history records at the three stations and the seismic intensities at the 168 stations in the study region. The SMGA model of case 2 had better fit to the time history records but overestimated the seismic intensities. Therefore, we propose an intermediate SMGA model of case 3 between the SMGA model of case 1 and that of case 2.

In this intermediate model, the SMGA areas and locations, rupture initiation locations, rupture timing, and stress drop are the same as in the case 2. We reduced the stress drop of the SMGA1 from 40 MPa to 30 MPa to improve the reproducibility of the seismic intensities, which were overestimated in Iwate-ken and Miyagi-ken. Table 3 lists the fault parameters for the SMGA model of case 3, and Figure 11 illustrates the fault model. The short-period level for this case is 2.36 E+20 Nm/s^2, which is 1.3 times larger than the

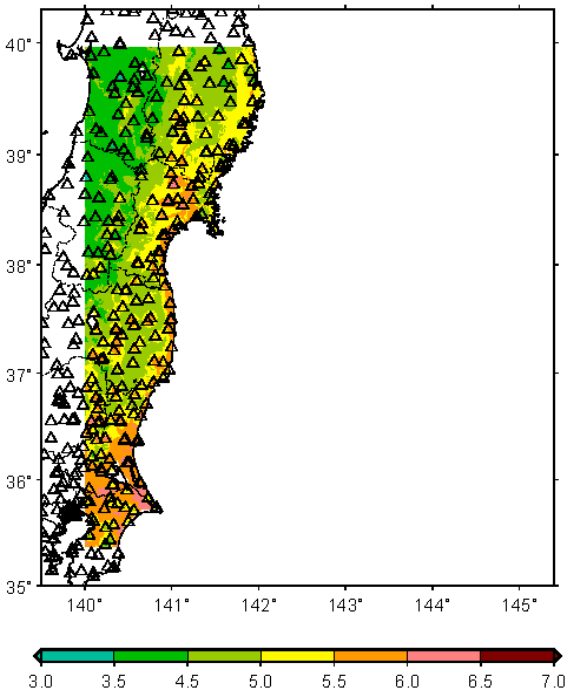

Fig. 6 – Observed seismic intensities of the records in the 2011 Tohoku earthquake.

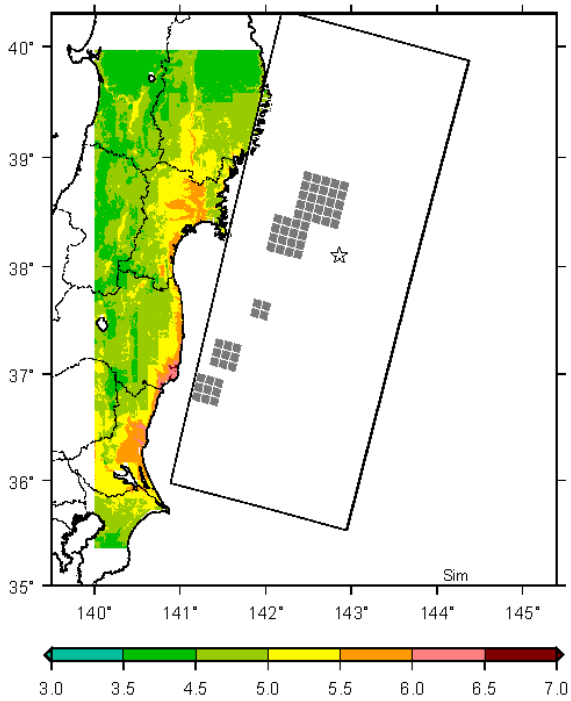

Fig. 7 – Seismic intensities calculated by the SMGA model of case 1.

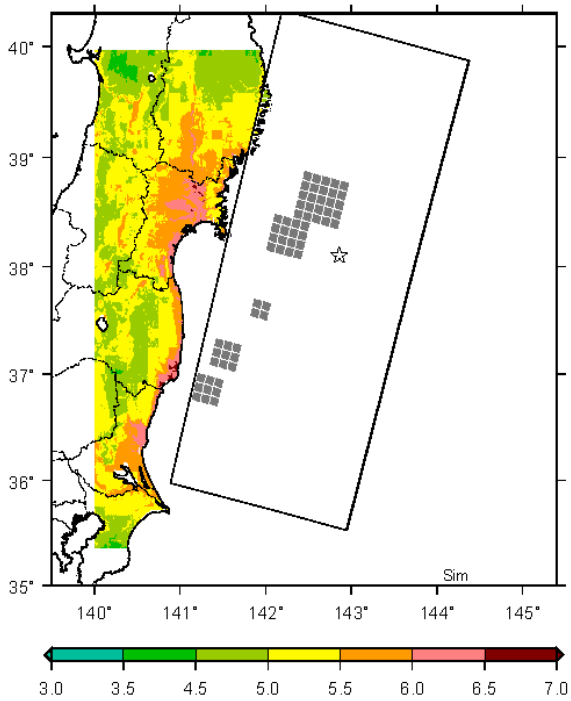

Fig. 8 – Seismic intensities calculated by the SMGA model of case 2.

empirical relationship between the seismic moment and the short-period level established for crustal earthquakes.

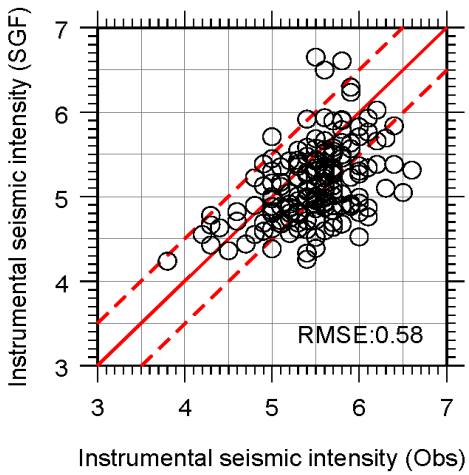

Fig. 9 – Comparison of the observed and calculated seismic intensities by the SMGA model of case 1.

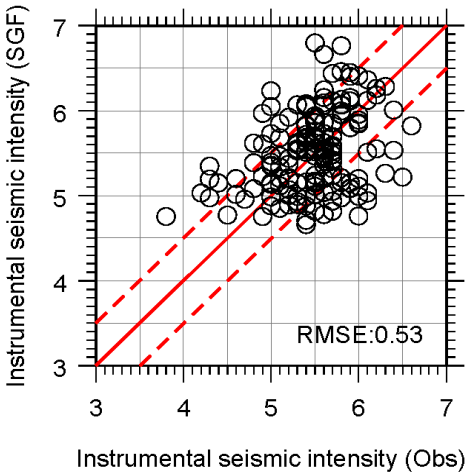

Fig. 10 – Comparison of the observed and calculated seismic intensities by the SMGA model of case 2.

5.2 Strong ground motion and seismic intensities

For case 3, we used the same Green's functions as for cases 1 and 2 depicted in Figure 11 as Events 1 to 4. The calculated strong motions by the stochastic Green's function method for case 3 are plotted in red in the Figures 3 to 5.

Because the stress drop was decreased only for SMGA1, the results show that the accelerations, velocities, and pseudo velocity response spectra of the simulated strong ground motion at MYGH12 station, which is close to SMGA1, decreased compared to the results of case 2, and were closer to the observation for NS and UD components than those of case 2, though EW component was still smaller than the observation. The results at FKSH17 and IBRH14 stations, which are far from the SMGA1, seem to have almost no change from case 2.

The seismic intensities of the results for the SMGA model of case 3 are plotted in Figure 12. The case 3 results show improvement of the seismic intensities in Iwate-ken and Miyagi-ken previously overestimated in case 2.

Furthermore, in Figure 13 the observed seismic intensities are compared with those simulated for the SMGA model of case 3 at the 168 stations used for the seismic intensity distribution. The simulated seismic intensities for case 3 show better correlation with the observation. The *RMSE* (Root Mean Square Error) of the observed seismic intensities and those simulated for the SMGA model of case 3 was 0.50, which was the smallest among the three cases.

From the above, the SMGA model of case 3 could reproduce well the strong motions at the three KiK-net stations, and the seismic intensity distribution for the SMGA model of case 3 was the most consistent with the observation in the study region. Therefore, we can conclude that the SMGA model of case 3 is the best case among the three cases.

6. Conclusions

This paper aims to facilitate the broadband ground motion prediction of future M_W 9-class events, by estimating the short-period level for the 2011 off the Pacific coast of Tohoku earthquake based on the SMGA models using the stochastic Green's function method.

For that, we examined three cases of the SMGA models for the 2011 off the Pacific coast of Tohoku earthquake, which were the SMGA model of case 1 based on Kawabe and Kamae (2013)[4], the SMGA model of case 2 based on Satoh (2012)[3], and the intermediate SMGA model of case 3.

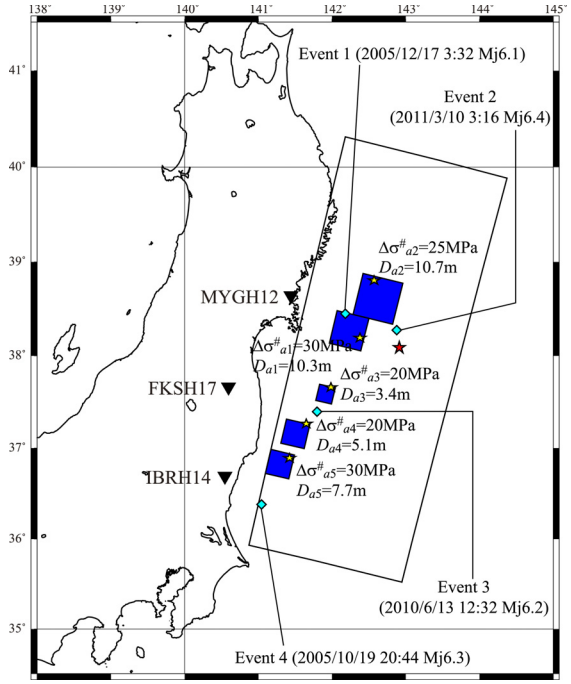

Fig. 11 – SMGA model of the case 3 for the 2011 Tohoku earthquake and the locations of the ground motion simulation stations. The stress drops on the SMGA 1 is turned from that in case 2.

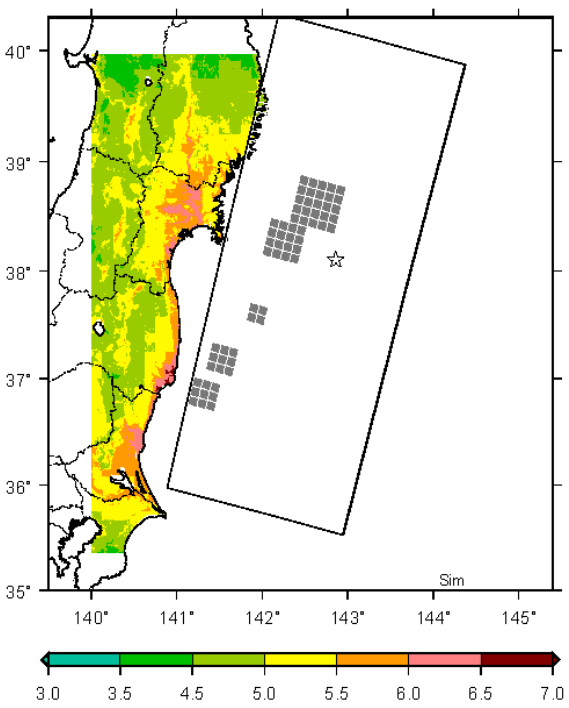

Fig. 12 – Seismic intensities calculated by the SMGA model of case 3.

Table 3 – Parameters of the SMGA model of case 3

SMGA	area S_i (km^2)	seismic moment M_0 (Nm)	slip D_i (m)	stress drop $\Delta\sigma_i$ (MPa)	short-period level A_i (N·m/s^2)
SMGA1	1600	7.88E+20	10.3	30	1.36E+20
SMGA2	2500	1.28E+21	10.7	25	1.42E+20
SMGA3	400	6.57E+19	3.4	20	4.54E+19
SMGA4	900	2.22E+20	5.1	20	6.81E+19
SMGA5	900	3.32E+20	7.7	30	1.02E+20
total					2.36E+20

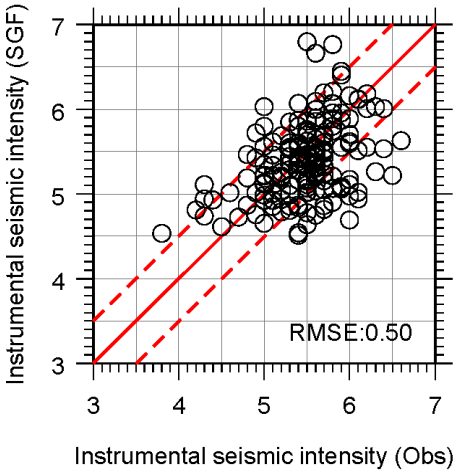

Fig. 13 – Comparison of the observed and calculated seismic intensities by the SMGA model of case 3.

The results showed that the strong motions calculated at three KiK-net stations (in Miyagi-ken, Fukushima-ken, and Ibaraki-ken) by the stochastic Green's function method for the SMGA model of case 1 underestimated the records and that those for the SMGA models of cases 2 to 3 had a better fit with the records. On the other hand, the seismic intensity distribution calculated from the stochastic Green's function analysis results for the SMGA model of case 3 was the most consistent with the observation.

Based on the above results, the short-period level of 2.36 E+20 Nm/s^2 for case 3, which was estimated by the stochastic Green's function method, is appropriate for the 2011 Tohoku earthquake. This value is 1.3 times larger than the empirical relationship between the seismic moment and the short-period level established for crustal earthquakes.

In this paper, we discussed the SMGA models for the 2011 off the Pacific coast of Tohoku earthquake. However, further study will be necessary for expanding the SMGA model to the asperity model with background area, as well as introducing the large-slip area and very-large-slip area to the fault model, which could represent the tsunami source.

7. Acknowledgements

This study includes the results of the research project in the fiscal year of 2018 by National Research Institute for Earth Science and Disaster Resilience, Japan.

8. References

[1] Headquarters for Earthquake Research Promotion (2005): Map of predicted earthquake ground motions in Japan. *Part 2, Explanation of the map of predicted earthquake ground motions with specified source faults* (in Japanese).

[2] Dan K, Watanabe M, Sato T, Ishii T (2001): Short-period source spectra inferred from variable-slip rupture models and modeling of earthquake faults for strong motion prediction by semi-empirical method. *Journal of Structural and Construction Engineering (Transactions of the Architectural Institute of Japan)*, **545**, 51-62 (in Japanese).

[3] Satoh T (2012): Source modeling of the 2011 off the Pacific coast of Tohoku earthquake using empirical Green's function method: From the viewpoint of the short period spectral level of interplate earthquakes. *Journal of Structural and Construction Engineering (Transactions of the Architectural Institute of Japan)*, **77**(675), 695-704 (in Japanese).

[4] Kawabe H, Kamae K (2013): Source modeling of the 2011 off the Pacific coast of Tohoku earthquake. *Journal of the Japan Association for Earthquake Engineering*, **13**(2), 75-87 (in Japanese).

[5] Kurahashi S, Irikura K (2013): Short-period source model of the 2011 M_W 9.0 off the Pacific coast of Tohoku earthquake. *Bulletin of the Seismological Society of America*, **103**(2B), 1373-1393.

[6] Satoh T (2010): Scaling law of short-period source spectra for crustal earthquakes in Japan considering style of faulting of dip-slip and strike-slip. *Journal of Structural and Construction Engineering (Transactions of the Architectural Institute of Japan)*, **75**(651), 923-932 (in Japanese).

[7] Headquarters for Earthquake Research Promotion (2004): Verification of strong ground motion prediction method using the observation records of the 2003 Tokachi-oki earthquake. https://www.jishin.go.jp/main/kyoshindo/pdf/20041220toka chi.pdf (Reference date 2019-1-21).

[8] Yoshida K, Miyakoshi K, Irikura K (2011): Source process of the 2011 off the Pacific coast of Tohoku earthquake inferred from waveform inversion with long-period strong-motion records. *Earth Planets Space*, **63**, 577-582.

[9] Ludwig WJ, Nafe JE, Drake CL (1970): Seismic refraction. *The Sea, New York*, **4**(1), 53-84.

[10] Dan K, Ju D, Muto M (2010): Modeling of subsurface fault for strong motion prediction inferred from short active fault observed on ground surface. *Journal of Structural and Construction Engineering (Transactions of the Architectural Institute of Japan)*, **75**(648), 279-288 (in Japanese).

[11] Boore DM (1983): Stochastic simulation of high-frequency ground motions based on seismological models of the radiated spectra. *Bulletin of the Seismological Society of America*, **73**(6), 1865-1894.

[12] Satoh T (2013): Short-period spectral level f_{max} and attenuation of outerrise, intraslab and interplate earthquakes in the Tohoku district. *Journal of Structural and Construction Engineering (Transactions of the Architectural Institute of Japan)*, **78**(689), 1227-1236 (in Japanese).

[13] Satoh T (2007): Attenuation of peak ground acceleration and peak ground velocity of statistical Green's function. *Journal of the Japan Association for Earthquake Engineering*, **7**(6), 1-16 (in Japanese).

[14] Headquarters for Earthquake Research Promotion (2017): Strong ground motion prediction method for earthquakes with specified source faults ("Recipe"). https://www.jishin.go.jp/main/chousa/17_yosokuchizu/recipe.pdf, (in Japanese) (Reference date 2019-1-21).

